

Spectral statistics of driven Bose-Hubbard models

Jesús Mateos, Fernando Sols, and Charles Creffield

Departamento de Física de Materiales, Universidad Complutense de Madrid, E-28040 Madrid, Spain

(Dated: April 16, 2024)

We study the spectral statistics of a one-dimensional Bose-Hubbard model subjected to kinetic driving; a form of Floquet engineering where the kinetic energy is periodically driven in time with a zero time-average. As the amplitude of the driving is increased, the ground state of the resulting flat-band system passes from the Mott insulator regime to an exotic superfluid. We show that this transition is accompanied by a change in the system's spectral statistics from Poisson to GOE-type. Remarkably, and unlike in the conventional Bose-Hubbard model which we use as a benchmark, the details of the GOE statistics are sensitive to the parity of both the particle number and the lattice sites. We show how this effect arises from a hidden symmetry of the Hamiltonian produced by this form of Floquet driving.

I. INTRODUCTION

In recent years Floquet engineering [1, 2] has become an increasingly important tool to control the dynamics of quantum systems. In this approach, a system is driven by a time-periodic perturbation, allowing its dynamics to be decomposed into two parts: a so-called micromotion oscillating at the same frequency as the driving, and an effective static Hamiltonian. In the limit of high frequency, the micromotion can frequently be neglected, and as a result the driven system can be simply described by just the effective Hamiltonian, the parameters of which can be controlled by varying the amplitude or phase of the driving. A typical example is controlling the tunneling of a particle in a lattice potential. By shaking the lattice periodically in time, the tunneling becomes renormalized [3], allowing it to be tuned [4] by altering the parameters of the shaking. In this way the effective tunneling can be set to zero to produce the effect known as coherent destruction of tunneling [5], to negative values to produce negative effective mass [6, 7], or can be rendered complex [8, 9] to simulate the effect of an applied magnetic field [10, 11].

This type of fine control over the parameters of the effective Hamiltonian allows the simulation [12, 13] of physical problems in which the effective Hamiltonian is engineered to mimic the Hamiltonian of another system [14–16], and also to encode problems in pure mathematics [17, 18]. The Floquet method is not only applicable at the single-particle level, but is also relevant to controlling strongly correlated systems. Regulating the effective tunnelling, for example, can be used to coherently induce the Mott transition in the conventional Bose-Hubbard model [19, 20] (see Fig. 1a). In many-body systems the periodic driving will eventually cause the system to heat up to infinite temperature [21–23]. It has been shown, however, that a generic system will first pass through a long-lived “pre-thermal” regime, in which the rate of heating is exponentially small in the driving frequency [24–28]. For high-frequency driving it is thus possible to manipulate the properties of a system using Floquet engineering while it remains in this prethermal state. Although in quantum simulation applications one is princi-

pally interested in the ground state of the effective Hamiltonian (such as whether it is an insulator or a superfluid), it is important to note that Floquet engineering affects the *entire* spectrum of the driven system, and so also controls the statistical distribution of the energy level spacings.

This distribution is frequently used to address the question of whether a system is integrable or chaotic. Berry and Tabor [29] conjectured that Poisson statistics would describe systems having an integrable classical limit, while conversely the Bohigas conjecture [30] indicates that systems with a semiclassical chaotic limit would be described by random matrix theory (RMT). Combining these results thus allows the spectral statistics to test whether a given system is chaotic (RMT) or integrable (Poisson). Quantum many-body systems, which do not necessarily possess a well-defined semiclassical limit, also seem to follow this rule in general [31], although some exceptions are known [32–34]. Depending on its symmetries, the spectrum of a quantum chaotic Hamiltonian will therefore be expected to fall into one of the three ensembles of RMT. In particular, if such a Hamiltonian possesses time-reversal symmetry, it should belong to the Gaussian orthogonal ensemble (GOE). This has been verified for a large number of many-body systems, including the Heisenberg, $t-J$, and fermionic Hubbard models [35, 36], the Bose-Hubbard model [37, 38], the ionic Hubbard model [39], and the SYK model [40].

In this work we study the statistics of the Floquet spectrum of the Bose-Hubbard model under kinetic driving [41], in which the hopping parameter is driven periodically in time with a zero time-average. This results in the suppression of first-order single-particle hopping, which places the setup in the class of flat-band systems, generally characterized by a vanishing single-particle group velocity. Other possible origins of flat-band behavior are frustration [42], spin-orbit coupling [43] and, importantly, the destructive interference between different paths in an elementary hopping process [44–49].

Just as in the case of the conventional Bose-Hubbard model, the ground-state of the system can be tuned to pass from a Mott insulator state to a superfluid, as shown in Fig. 1b, as the driving parameter is varied. The re-

II. MODELS

The conventional Bose-Hubbard (BH) model is given by the Hamiltonian

$$H_{\text{BH}} = -J \sum_{\langle i,j \rangle} (a_i^\dagger a_j + H.c.) + \frac{U}{2} \sum_j n_j (n_j - 1), \quad (1)$$

where J is the hopping amplitude, a_j/a_j^\dagger are bosonic annihilation/creation operators for a particle on site j , n_j is the standard number operator $n_j = a_j^\dagger a_j$, and U is the Hubbard repulsion (that is, we take U to be positive). The behavior of the model is dictated by the competition between the kinetic energy, regulated by J , and the interparticle repulsion U . For the case of commensurate filling, when the number of bosons is an integer multiple of the number of sites, the eigenstates of the system are approximately Fock states in the limit $U \gg J$. In particular the ground state consists of bosons that are highly localized in space, forming a Mott insulator. As shown in Fig. 1a, the corresponding momentum density is flat. When J/U is increased, the bosons are able to delocalise and the phase-coherence of the state increases. As a result a crossover from the Mott state to a superfluid [52] occurs at a critical coupling [53] of $J/U_c \simeq 0.2$. This is marked by a sharp peak forming at $k = 0$ in the momentum density, indicating the formation of a macroscopically-occupied zero momentum-state. For convenience we shall henceforth label these two regimes by the character of the ground state of the commensurate system, and term them the ‘‘Mott regime’’ and the ‘‘superfluid regime’’ respectively. An additional regime occurs in the limit $U \ll g$ when the system evolves towards a gas of free bosons, which differs from a conventional superfluid in certain physical aspects [51].

A. Floquet theory

A quantum system whose Hamiltonian varies periodically with time, $H(t) = H(t + T)$ where T is the period of the system, can be described efficiently in terms of Floquet theory. Such a time-dependent Hamiltonian can arise, for example, if the system is driven by an oscillating external field, or if a parameter of H is periodically varied in time. We seek solutions of the time-dependent Schrödinger equation $[H(t) - i\hbar\partial_t]\phi_n(t) = \epsilon_n\phi_n(t)$. The eigenfunctions $\phi_n(t)$ are T -periodic functions of time termed Floquet states, while the eigenvalues ϵ_n are generalizations of the energy eigenvalues obtained in static systems, and are termed Floquet quasienergies. This type of solution is familiar in the context of solid state physics, where *spatial* periodicity allows spatial wavefunctions to be written in terms of Bloch states and quasimomenta (Bloch’s theorem). It should be noted that the quasienergies are only defined up to integer multiples of the driving frequency ω , and so similarly to the case of quasimomentum, the quasienergy has a Brillouin zone structure.

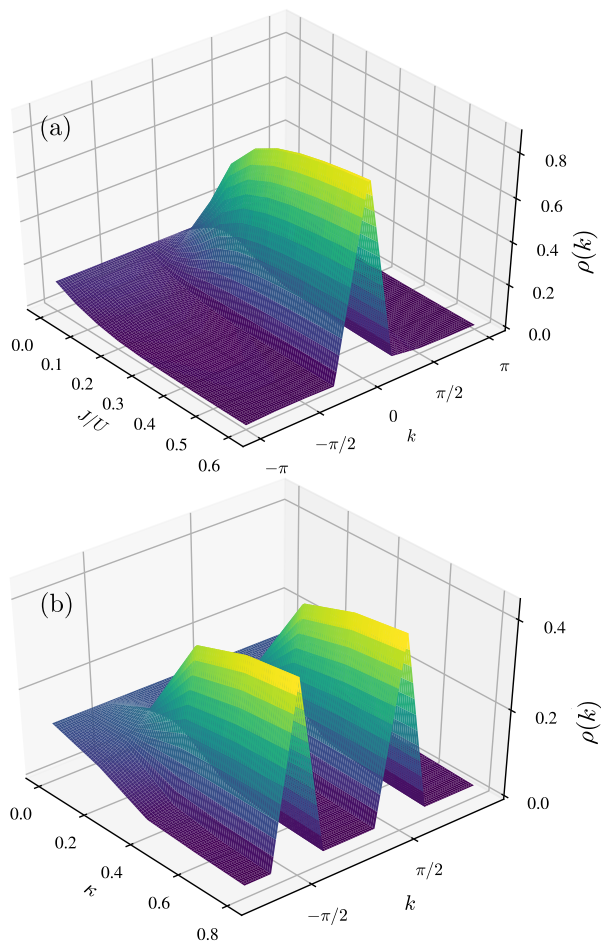


FIG. 1. The single-particle momentum density of the ground state of the Bose-Hubbard model. (a) For small J/U the ground state of the conventional BH model is a Mott insulator, and the momentum density is flat. As J/U is increased the system becomes superfluid, and a single peak develops at zero momentum. (b) Kinetic driving. At low values of κ the system is again a Mott insulator with a uniform momentum density. For larger κ the system makes a transition to an exotic superfluid, characterized by the occupation of *two* momentum states, $k = \pm\pi/2$. Parameters: 8 sites, 8 particles.

sulting superfluid, however, is rather exotic due to the unusual pairing correlations induced by the driving, and consists of a cat-like superposition of two many-body states of opposite momentum [50, 51]. We will show that these unusual pairing effects not only manifest in the ground-state properties of the system, but also in the spectral statistics of the model. Moreover, they are associated with a discrete symmetry non-existent in the undriven system. As a result, and unlike the conventional Bose-Hubbard model, the spectral statistics become sensitive to the parities of the number of particles in the system and the number of lattice sites. When this symmetry is absent, the statistics is described by a single GOE, but by a mixture of two GOEs when it is present.

The Floquet states provide a complete basis, and so the time evolution of a general quantum state can be expressed as

$$\psi(t) = \sum_n c_n e^{-i\epsilon_n t} \phi_n(t), \quad (2)$$

analogous to the standard expansion of a wavefunction in energy eigenstates of a static Hamiltonian. In the limit of high frequency, we can see that a separation of energy scales is present in this expression. The Floquet states have the same periodicity as $H(t)$, and so in this limit frequencies they only produce structure over short timescales – the so-called “micromotion”. In contrast, behaviour on timescales much longer than T are essentially determined by just the quasienergies. In this limit we can thus consider the dynamics to be given simply by an effective static Hamiltonian, H_{eff} , whose eigenvectors and eigenvalues correspond to the Floquet states and quasienergies respectively.

It is usually difficult, however, to obtain analytical expressions for this effective Hamiltonian. A common approach is to make an expansion in inverse powers of the frequency

$$H_{\text{eff}} = \sum_{j=0}^{\infty} \frac{1}{\omega^j} H_{\text{eff}}^{(j)}, \quad (3)$$

such as the Magnus [54] or van Vleck [55] series. If this expansion is well-defined and stable, then one can obtain a high-frequency approximation to H_{eff} by truncating it to the lowest-order terms. This approximation will become progressively more accurate as ω is increased.

B. Potential driving

To introduce the technique of Floquet engineering, we first consider the well-studied case of when the Hamiltonian is modified by a time-dependent potential. By periodically accelerating and decelerating the lattice in space, or “shaking” it, the Bose-Hubbard Hamiltonian (1) seen in the rest frame of the lattice acquires a time-dependent term, $H(t) = H_{\text{BH}} + V(t)$, where the time-dependent potential is given by

$$V(t) = K \cos \omega t \sum_j n_j, \quad (4)$$

K being the amplitude of the shaking and ω is its frequency. By transforming to the interaction picture and averaging over one period of the driving, one obtains an effective Hamiltonian [19] valid in the limit of high driving frequencies ($\omega \gg U, J$) identical to Eq. 1, but with a renormalized tunneling parameter $J \rightarrow J \mathcal{J}_0(K/\omega)$, where \mathcal{J}_0 is the zeroth Bessel function of the first kind.

The process of Floquet engineering then consists of adjusting the parameters of the driving, K and ω , to regulate the amplitude of the effective tunneling. In this

way the value of J/U can be tuned [56] across the Mott-superfluid transition, without addressing the lattice parameters directly. In particular, if the driving is tuned to $K/\omega \simeq 2.404$ – the first zero of the Bessel function – the effective tunneling vanishes and the system becomes a Mott insulator.

C. Kinetic driving

In principle any term in (1) can be periodically driven to obtain an effective Hamiltonian in the high-frequency limit. Here we will consider the specific case of “kinetic driving” in which the tunnelling parameter, J , is periodically oscillated with zero time-average

$$J(t) = J \cos \omega t. \quad (5)$$

A scheme for producing a driving of this type in experiment was described in Ref. [41].

To obtain the effective Hamiltonian corresponding to this form of driving, it is advantageous to work in a momentum representation. In momentum space the conventional BH model (1) can be written as

$$H_{\text{BH}} = -2J \sum_{\ell=0}^{L-1} \cos(k_\ell) a_{k_\ell}^\dagger a_{k_\ell} + \frac{U}{2L} \sum_{\ell, m, n, p=0}^{L-1} \delta_{k_\ell + k_m, k_n + k_p} a_{k_p}^\dagger a_{k_n}^\dagger a_{k_m} a_{k_\ell}, \quad (6)$$

where the momenta run over the first Brillouin zone (FBZ) $k_\ell = 2\pi\ell/L$, $\ell \in \mathbb{Z}$ and L is the number of lattice sites. Performing the same form of Floquet analysis as before [41] yields the effective Hamiltonian

$$H_{\text{eff}} = \frac{U}{2L} \sum_{\ell, m, n, p=0}^{L-1} \delta_{k_\ell + k_m, k_n + k_p} \times \mathcal{J}_0[2\kappa F(k_\ell, k_m, k_n, k_p)] a_{k_p}^\dagger a_{k_n}^\dagger a_{k_m} a_{k_\ell}, \quad (7)$$

where $\kappa = J/\omega$ is the driving parameter, and

$$F(k_\ell, k_m, k_n, k_p) = \cos(k_\ell) + \cos(k_m) - \cos(k_n) - \cos(k_p). \quad (8)$$

We will term this Hamiltonian the kinetically-driven BH model. Note that since this Hamiltonian was derived in the high-frequency limit, the driving parameter κ is necessarily limited to the range $\kappa < 1$.

This effective Hamiltonian constitutes the lowest-order term in an expansion in orders of $1/\omega$ (Eq. 3). In principle, higher-order terms could also be derived. However, in the limit $1/\omega \rightarrow 0$ in which we work, their influence is small, and can be rendered negligible by raising ω sufficiently. It is straightforward to calculate the true quasienergies of the driven BH model numerically by diagonalizing the time-evolution operator for one period,

$U(T, 0)$

$$U(T, 0) = \mathcal{T} \left(\exp \left[-i \int_0^T H(t') dt' \right] \right) \quad (9)$$

where \mathcal{T} is the time-ordering operator. The eigenvalues of $U(T, 0)$, $\{\lambda_j\}$, are simply related to the quasienergies via $\lambda_j = \exp[-iT\epsilon_j]$. In Fig. 2 we compare the energy levels of H_{eff} with the true quasienergies as the driving frequency is increased. For the two cases shown, it can be clearly seen that for $\omega/U > 50$, the eigenvalues of H_{eff} coincide with the Floquet quasienergies to an accuracy of better than 0.1%. Furthermore, the differences between the energy levels and quasienergies scale quite accurately as $(U/\omega)^2$. We have further verified that the same scaling occurs for the complete energy spectrum over the entire range of κ . This confirms that H_{eff} is indeed an accurate and well-controlled approximation to the full Floquet operator in both the Mott insulator and superfluid regimes, and that H_{eff} becomes exact in the limit $\omega \rightarrow \infty$.

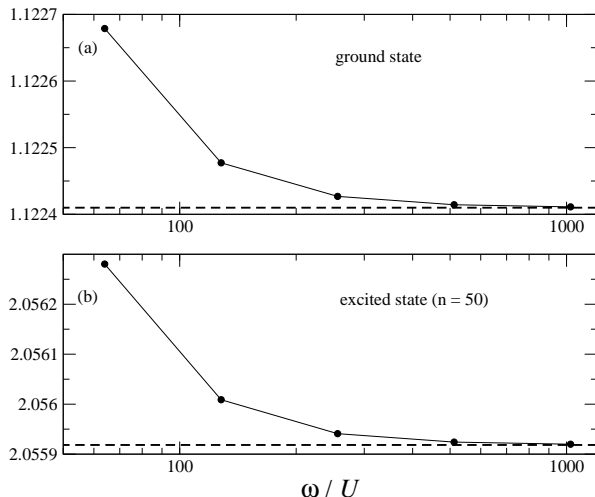


FIG. 2. Representative quasienergies of the kinetically-driven BH model obtained from the exact diagonalization of the full Floquet Hamiltonian, compared with the results of the effective Hamiltonian (7). (a) Ground state. As the frequency, ω of the driving is increased, the lowest quasienergy monotonically approaches the ground state energy of the effective model, the difference reducing as $(U/\omega)^2$. (b) As in (a) but for an arbitrarily chosen excited state ($n = 50$). As before the quasienergy of the kinetically-driven BH model asymptotically approaches that predicted by the effective model as $(U/\omega)^2$. Clearly the effective model becomes exact in the limit $\omega \rightarrow \infty$. Parameters: 8 sites, 8 particles, $\kappa = 0.3$. Energies measured in units of J .

In contrast to the case of potential driving, we see that there are no single-particle hopping terms in this

(N, L)	$\dim(\mathcal{H})$	$\dim(\mathcal{H}_0)$	$\dim(\mathcal{H}_0^+)$
(7, 8)	3432	429	232
(8, 8)	6435	810	440
(9, 8)	11440	1430	750
(8, 9)	12870	1430	750
(9, 9)	24310	2740	1387
(10, 11)	184756	16796	8524
(11, 11)	352716	32066	16159
(11, 12)	705432	58786	29624
(12, 12)	1352078	112720	56822

TABLE I. Dimension of the Hilbert space \mathcal{H} and its subspaces. We label the system by (N, L) where N is the number of bosons and L is the number of lattice sites. \mathcal{H}_0 denotes the subspace of zero-momentum states, while \mathcal{H}_0^+ signifies the subspace of states with both zero momentum and reflection symmetry. The dimension of \mathcal{H} is simply given by the binomial coefficient $\dim(\mathcal{H}) = \binom{N+L-1}{N}$; the other dimensions are obtained numerically by counting states.

effective Hamiltonian. Instead, the dynamics arises from four-operator terms, such as the motion of doublons and assisted tunneling processes [57]. As a consequence the motion of particles is highly correlated, producing a novel type of flat-band system. When the driving parameter κ is set to zero, the ground state of the model for commensurate filling is again a Mott insulator [41]. As κ is increased, the system makes a transition to an exotic superfluid state [50, 51]. Just as with the conventional BH model, we will label these two regimes of the kinetically-driven BH model by the behaviour of the ground-state of the commensurate system, so that low- κ corresponds to the Mott regime, and high- κ to the superfluid. As shown in Fig. 1b, in the superfluid regime the momentum density shows two peaks, indicating the macroscopic occupation of two momentum states, $k = \pm\pi/2$. Reference [50] showed that the ground state is actually a cat-like superposition of these two many-particle momentum states, and uncovered the particular importance of the two-particle scattering processes $(k, \pi - k) \rightarrow (k', \pi - k')$, which energetically favor the occupation of these momenta.

III. RESULTS

To obtain the energy levels of the Hamiltonians (6) and (7), we employ an exact diagonalization method, working in a momentum-space basis. In all cases we apply periodic boundary conditions. The Hamiltonians possess a number of discrete symmetries such as momentum conservation and parity symmetries, and in order to investigate the spectral statistics of the system it is necessary to study each subspace separately. Following Ref. [38]

we work in the subspace of states with translation invariance, $a_j \rightarrow a_{j+1}$ in real space, which is equivalent to considering states of zero total momentum, and reflection symmetry $a_k \rightarrow a_{-k}$ in momentum space. In Table I we give the dimensions of the Hilbert spaces and subspaces obtained by imposing these symmetries for systems of N bosons in an L -site lattice, which we shall denote as (N, L) . Note that imposing these two symmetries considerably reduces the size of the Hilbert space, allowing the diagonalization of systems as large as $(12, 12)$ on a standard desktop computer.

A. Energy level spacings

The most direct way to study the spectral statistics of a system is to look at the spacings between consecutive energy levels, $s_n = E_{n+1} - E_n$. Following the Berry-Bohigas conjectures, for an integrable system the probability that a normalized spacing lies between s and $s + ds$ should be given by the Poisson distribution

$$P(s) = e^{-s}, \quad (10)$$

while in contrast, chaotic systems should exhibit GOE statistics

$$P(s) = \frac{\pi s}{2} e^{-\pi s^2/4}. \quad (11)$$

The level spacings will have a smoothly varying component depending on the local density of states, and fluctuations around this smooth behavior. It is these fluctuations which are expected to have the universal behaviour described by Poisson statistics or RMT. It is thus necessary to first remove the smooth part, a procedure which is known as ‘‘unfolding’’. For some systems, such as billiards, the smooth behavior is known analytically, but in general the choice of smooth function is somewhat arbitrary and can influence [58] the results.

In Fig. 3 we show the histograms obtained for the conventional BH model for a large $(12, 12)$ system at a low and a high value of J/U . In both cases we used a fitted cubic polynomial to perform the unfolding. In the limit $J/U \rightarrow 0$, the system will be in the Mott regime and so will be trivially integrable. Accordingly we see in Fig. 3a that the level spacings histogram for the lower value of $J/U = 0.01$ has a strikingly Poissonian form, peaked at zero with an exponential decay. As J/U is increased, the system will leave the Mott regime and enter the more weakly-interacting superfluid regime. In this regime the distribution of level spacings shown in Fig. 3b has GOE form. In particular we can note the suppression of the distribution for $s \simeq 0$, indicating the development of avoided crossings in the spectrum, and thus the presence of quantum chaos. Similar results are also obtained for the $(11, 12)$ case (not shown).

In Fig. 4 we show the equivalent histograms for the kinetically-driven BH model. For a low value of the driving parameter, $\kappa = 0.1$ the system will be in the Mott

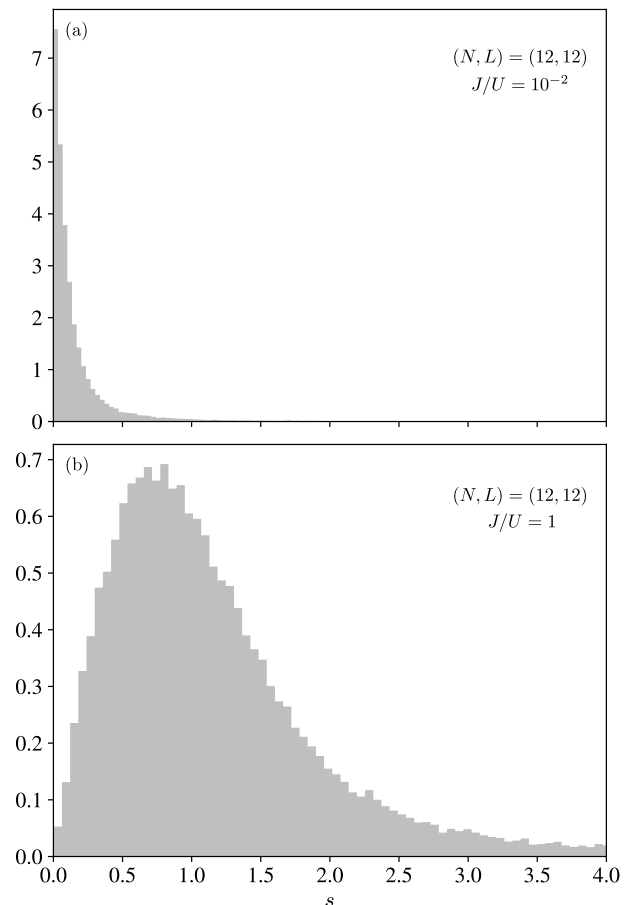


FIG. 3. Histograms of normalized level spacings for the conventional BH model. (a) For $J/U = 10^{-2}$ the system is in the Mott regime, and the spacings show a clear Poisson distribution (Eq. 10). (b) For $J/U = 1$ the system is in the superfluid regime, and the spectral statistics change to GOE form (Eq. 11). In particular, note the suppression of spacings for $s \simeq 0$, indicating the presence of avoided crossings and thus quantum chaos. In both cases the system size is $(12, 12)$.

regime, and just as before the histograms indeed show a Poisson distribution (Figs. 4a and b). Like H_{BH} , H_{eff} is also a hermitian operator with time-reversal symmetry, and so we expect its spectral statistics also to be described by the GOE [59] away from the integrable limit. In Fig. 4c we see that for the case of $(11, 12)$ (11 bosons on a 12-site lattice) the distribution indeed changes to GOE form as κ is increased, and the system passes from the Mott to the superfluid regime. For the $(12, 12)$ case, however, the behaviour for large κ is less clear (Fig. 4d). While the distribution is not Poissonian, it shows less suppression for $s \simeq 0$ than the GOE distribution, and appears to be intermediate between these two distributions. To investigate this behaviour, and to obtain more quantitative estimates for the spectral distributions, we will now proceed to analyze the statistics of the gap-ratios.

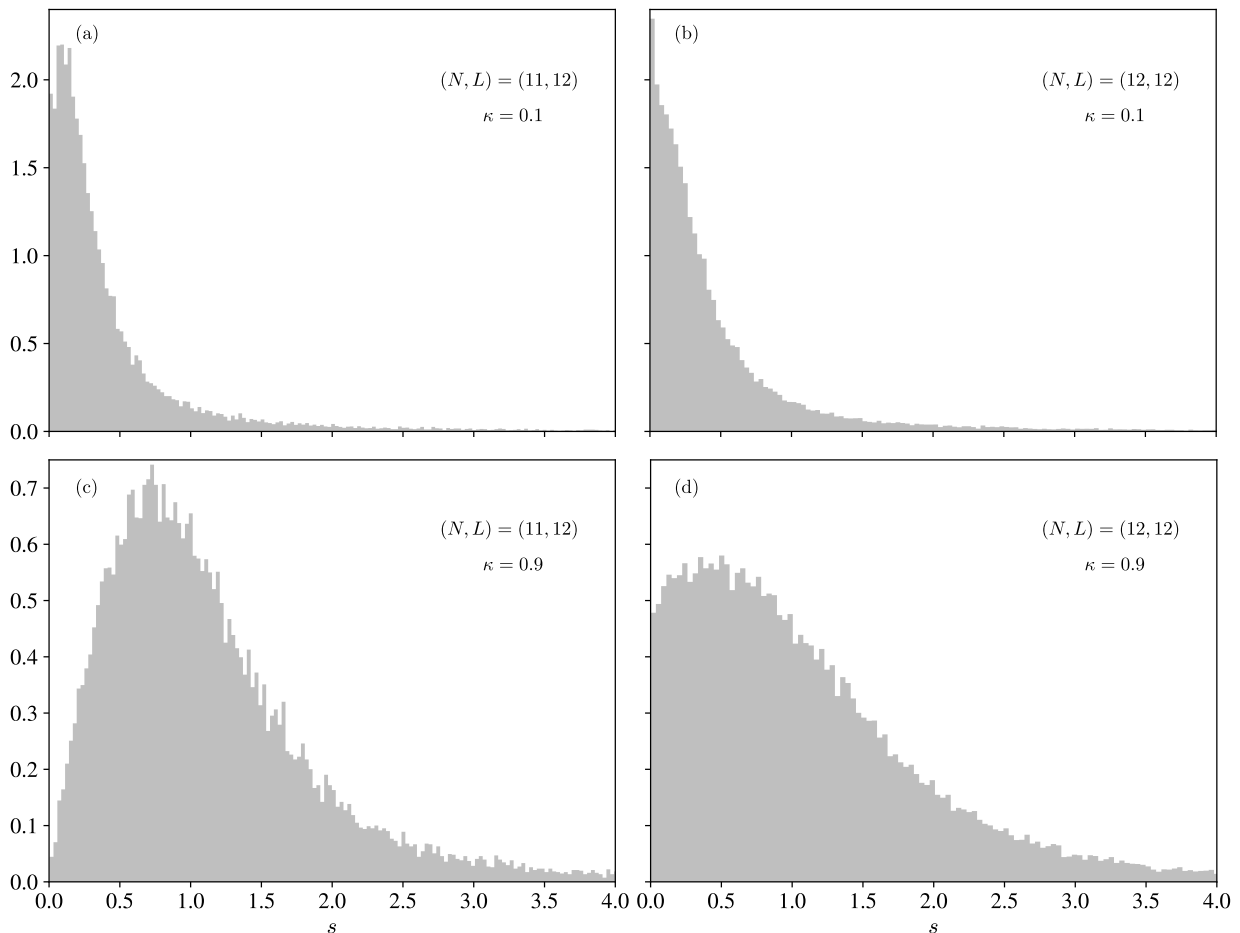


FIG. 4. Histograms of normalized level spacings for the kinetically-driven BH model. (a) For $\kappa = 0.1$ the $(11, 12)$ system is in the Mott regime, and its energy spacings are Poisson distributed. (b) Similarly, the $(12, 12)$ system is also Poissonian for $\kappa = 0.1$. (c) For $\kappa = 0.9$, the $(11, 12)$ system is in the superfluid regime and the statistics become GOE. (d) Unlike in (c), the $(12, 12)$ system does not exhibit GOE statistics in the superfluid regime. Instead the distribution appears to be intermediate between Poisson and GOE.

B. Gap ratios

The ratio of consecutive gaps is defined as

$$r_n = \min\left(\frac{s_{n+1}}{s_n}, \frac{s_n}{s_{n+1}}\right). \quad (12)$$

This quantity was introduced by Oganesyan and Huse [60], and has the advantage that its measurement does not require the unfolding procedure, as the ratio of consecutive spacings does not depend on the local density of states. The statistical distribution of r is straightforward to obtain for the Poisson case

$$P(r) = \frac{2}{(1+r)^2}, \quad (13)$$

and Wigner-like surmises have been obtained [61, 62] for the RMT ensembles.

We show results for the conventional BH model in Fig. 5. The results corroborate the behaviour seen previously

in the gap spacings: the Mott insulating system obtained for low J/U exhibits clear Poissonian statistics, while the superfluid case, obtained for $J/U = 1$, exhibits GOE statistics. The excellent agreement between the numerics and the analytical results is quite striking, and underlines the power of using spectral analysis to discriminate between integrable and quantum chaotic systems.

In Fig. 6 we show the analogous results for the kinetically-driven BH model for the two system sizes considered previously. Similarly to the case of the conventional BH model, the distribution of gap-ratios for the $(11, 12)$ system (Fig. 6a and c) changes from Poisson to GOE statistics as the system passes from the Mott regime to the superfluid. Again, however, the $(12, 12)$ (Fig. 6b and d) exhibits an unusual behaviour: in the strongly-correlated regime the gap-ratios have a Poissonian distribution as expected, but in the superfluid regime the distribution is neither Poisson nor GOE. Rather, as we will discuss later, it seems to fit a distribution of two mixed GOEs.

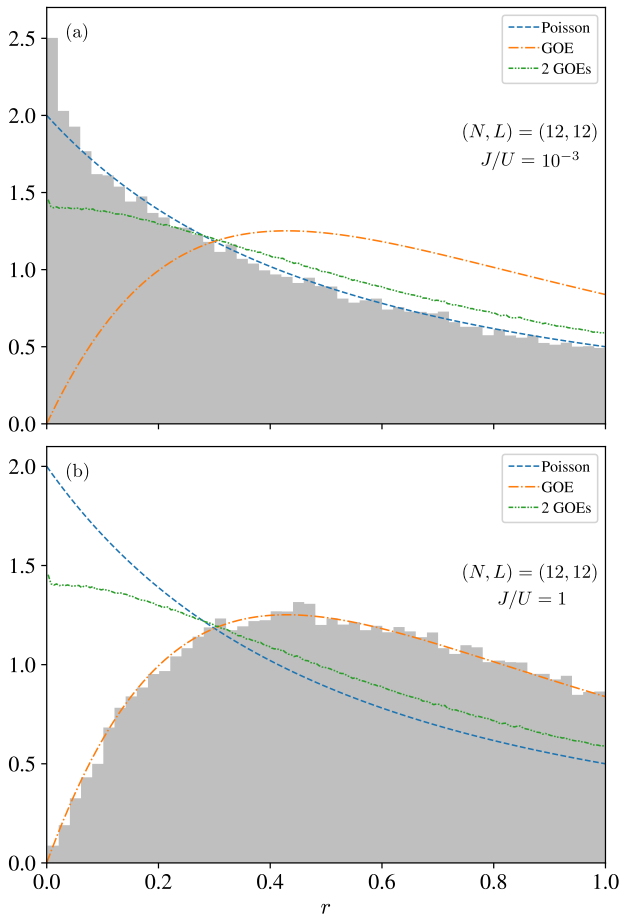


FIG. 5. Histograms of the gap-ratios for the conventional BH model. (a) In the Mott insulator regime, $J/U = 10^{-3}$, the gap-ratios arise from a Poissonian distribution of level spacings (Eq. 13). (b) For $J/U = 1$, in the superfluid regime, the distribution of gap-ratios is well-described by the GOE, in agreement with the previous results for the level spacings. In both cases the system size is $(12, 12)$.

From their statistical distributions it is straightforward to calculate the mean gap-spacing, $\langle r \rangle$, which can be used to quantitatively assess to which statistical ensemble a given spectrum belongs. For the Poisson distribution, $\langle r \rangle_{\text{Poi}} = 2 \log 2 - 1 \simeq 0.386$, while for the GOE case $\langle r \rangle_{\text{GOE}} \simeq 0.528$ [63]. In Fig. 7 we plot the values of $\langle r \rangle$ for the conventional and kinetically-driven BH models for several different choices of boson-number and system size, as we vary the driving parameters. In each case the size of the error bars was estimated by making a bootstrap over 4,000 resamples.

The case of the conventional BH model is straightforward to interpret. This model is integrable in two extremes; for the Mott limit, as we have already seen, when $J/U \rightarrow 0$, and also in the limit $J/U \rightarrow \infty$ when the system becomes a free boson gas. Accordingly we can see in Fig. 7a that $\langle r \rangle$ takes a value close to that arising from Poissonian statistics at these limits. As was pre-

viously seen in Ref. [38], some variation from the Poissonian value of $\langle r \rangle$ is visible, especially for the smaller system sizes. In the Mott limit this is a consequence of the difficulty of calculating the statistics of a spectrum consisting of well-separated clusters of nearly degenerate energy levels. For intermediate values of J/U the value of $\langle r \rangle$ saturates to a value close to the GOE average, indicating that the conventional superfluid exhibits quantum chaos [37, 38]. We observe only minor dependence on the system size, with the width of the GOE region slightly broadening as the system size increases, but no dependence on the parities of N and L .

Integrability is a fragile property, and so one might expect the spectral statistics to abruptly change from Poisson to GOE as soon as the system is tuned away from an integrable point. Instead Fig. 7a shows a rather smooth crossover between the limits. Whether the GOE region continues to broaden, thereby making the transition become sharper as the system approaches the thermodynamic limit remains an open question, and would require the study of even larger systems. As we can see from Table I, however, the rapid growth in the size of the Hilbert space as N and L are increased make addressing this question extremely challenging.

As we have seen previously, however, the results for the kinetically-driven BH model are more difficult to interpret. Unlike the conventional BH model, the system only passes through a single phase transition as the driving parameter is varied. For small κ all the system sizes considered exhibit Poisson statistics, corresponding to the integrability of the model in this limit. As κ is increased, we again see that $\langle r \rangle$ smoothly increases away from this value, similarly to the behaviour seen in the conventional BH model. At a critical value of κ the system makes a transition to the superfluid state, but unlike in the conventional BH case, we do observe a clear dependence on the parities of N and L of $\langle r \rangle$ in this regime. When both the particle number and the number lattice sites are even, $\langle r \rangle$ approaches a value intermediate between the Poisson and GOE values, and otherwise $\langle r \rangle$ approaches the GOE value.

Obtaining statistics intermediate between GOE and Poisson is characteristic of systems containing a hidden symmetry. In principle identifying this symmetry would allow the Hamiltonian to be divided into independent blocks, each of which would individually be described by RMT. Refs. [64, 65] calculated the statistics for systems composed of several sub-blocks, and we show the gap-ratio distributions for several examples in Fig. 8. For a single GOE, the gap-ratios show the characteristic suppression for small r , arising from level repulsion, indicating the presence of quantum chaos. For the case of two mixed GOEs, however, this feature vanishes, and the resulting distribution is more similar to, but clearly distinct from, a Poisson distribution [35]. This tendency continues as the number of mixed GOEs increases, and indeed as the number of mixed spectra approaches infinity, the distribution tends towards Poisson [65].

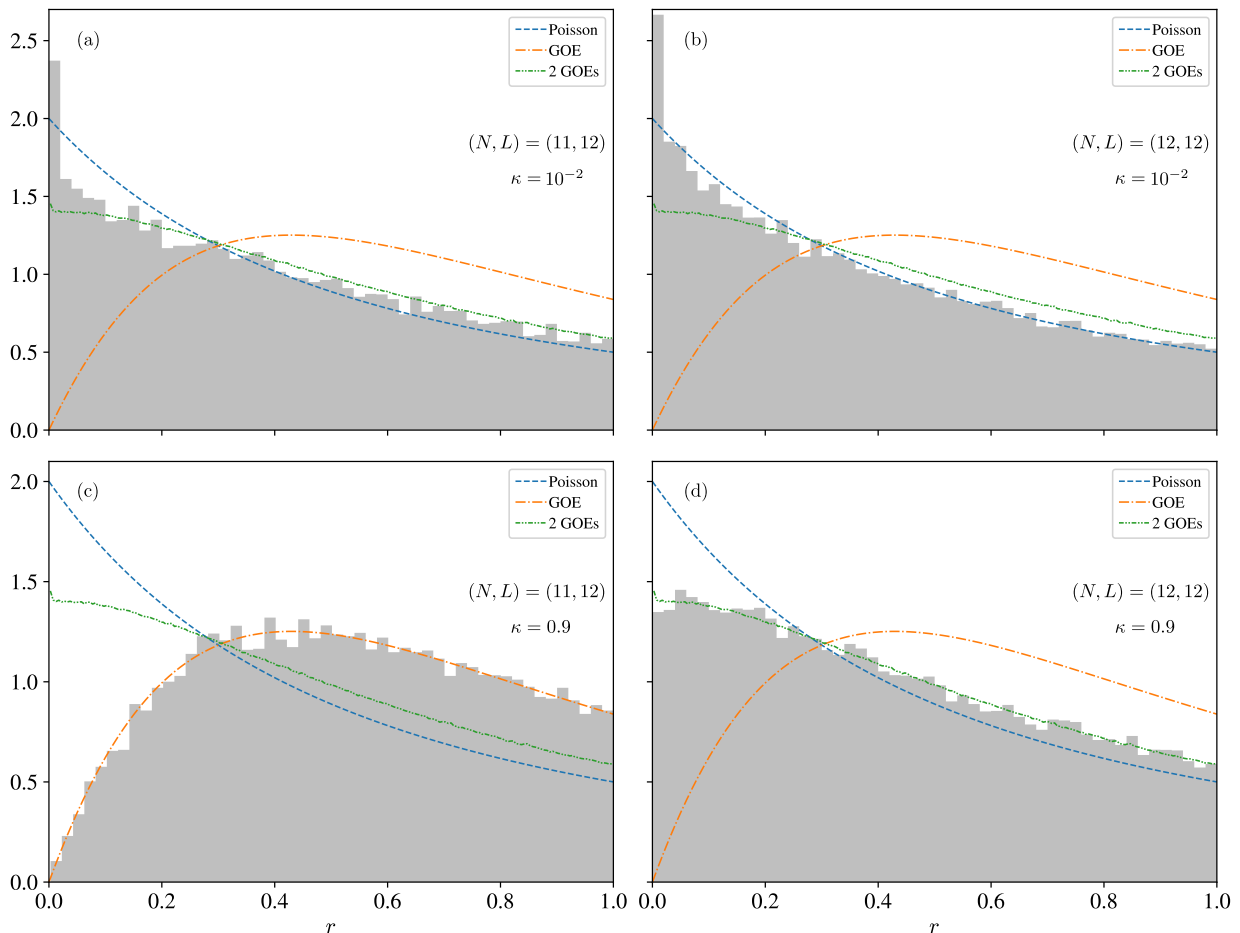


FIG. 6. Histograms of the gap ratios for the kinetically-driven BH model. (a) For $\kappa = 0.01$ the $(11, 12)$ system is in the Mott regime and the distribution of gap-ratios is well-described by the Poisson result. (b) Similarly, the $(12, 12)$ system is also Poissonian for $\kappa = 0.1$. (c) For $\kappa = 0.9$, the $(11, 12)$ system makes a transition to the superfluid regime and the statistics of the gap-ratios is again GOE. (d) Unlike in (c), the $(12, 12)$ system does not follow simple GOE statistics in the superfluid regime. Instead the distribution is described accurately by a mixture of two GOEs.

The value obtained for $\langle r \rangle$ for the $(8, 8)$ and $(12, 12)$ agrees well with that obtained for two mixed GOEs [65], $\langle r \rangle = 0.423$, as can be seen from Fig. 7b. To verify this further, the statistical distribution of the gap-ratios is also plotted in Fig. 6, and again the agreement is seen to be excellent, particularly in the high- κ limit. Thus for the kinetically-driven BH model we see two types of spectral statistics in the superfluid regime: a single GOE in general, but two mixed GOEs when N and L are both even. Additional examples for different values of N and L are given in the Appendix.

C. Hidden symmetry

The study of the gap-ratios clearly indicates that the spectral statistics of the kinetically-driven BH model when both N and L are even are described by a mixture of two GOEs in the superfluid phase. This points to the

presence of an additional symmetry in the kinetically-driven BH Hamiltonian beyond the translation and reflection symmetries already accounted for, which depends on the parities of N and L . Furthermore this symmetry must arise from the kinetic driving, as it is not present in the undriven BH model.

As noted previously, an essential property of the kinetically-driven BH model is the importance of pairing correlations between momenta π and $\pi - k$. If we define the π -reflection transformation, \mathcal{R}_π , as

$$\mathcal{R}_\pi : a_k \rightarrow a_{\pi-k} . \quad (14)$$

it is straightforward to show that the kinetically-driven BH Hamiltonian is *exactly* invariant under this transformation for all k , while the conventional BH model is not. In addition, under this transformation, the total momen-

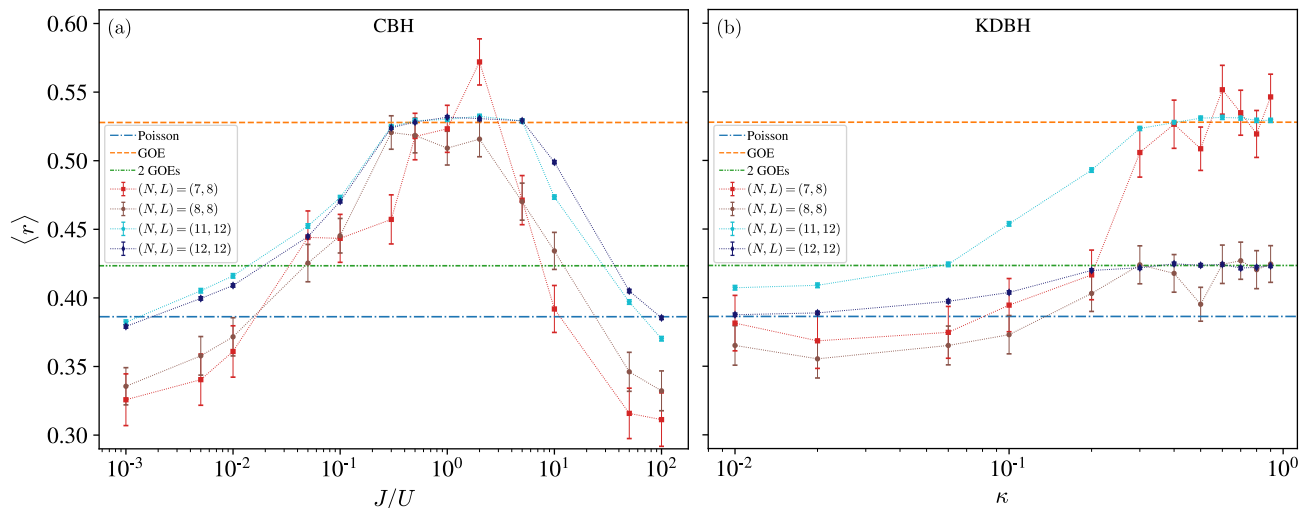


FIG. 7. Mean gap-ratio $\langle r \rangle$ as a function of the control parameter. (a) Conventional Bose-Hubbard model (CBH). This model admits two integrable limits: $J/U \rightarrow 0$ when the system tends to a Mott insulator, and $J/U \rightarrow \infty$ when it describes a gas of free bosons. In both cases $\langle r \rangle$ indicates that the spectral statistics are Poissonian. Between these limits, in the superfluid regime, the statistics are GOE. Strong dependence on particle number or system size is not evident. (b) Kinetically-driven BH (KDBH). For small κ , in the Mott regime all the system sizes have a Poissonian distribution. In the superfluid regime, however, two different behaviors are evident. For (7, 8) and (11, 12) the statistics becomes GOE, just as seen in the conventional BH model. For (8, 8) and (12, 12), $\langle r \rangle$ tends to a value characteristic of a mixture of two GOEs, $\langle r \rangle = 0.423$, indicating that these systems have an additional internal symmetry.

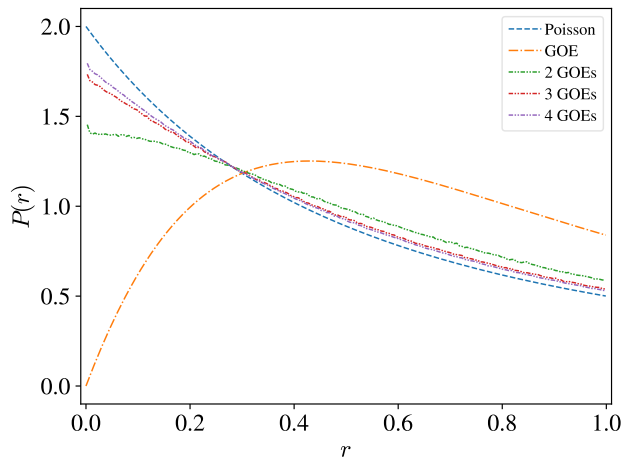


FIG. 8. Distribution of gap-ratios for several different cases: Poisson and GOE, and then from the mixture of two, three and four GOE matrices. The GOE distribution shows the characteristic suppression for small r , indicating the presence of quantum chaos. The mixed results do not show this feature, and rapidly approach the Poisson result as the number of independent GOE matrices is increased.

tum of the system transforms as

$$Q \rightarrow \tilde{Q} = \sum_{\ell=0}^{L-1} (\pi - k_{\ell}) n_{k_{\ell}} = \pi N - Q. \quad (15)$$

From this it is clear that the π -reflection symmetry is

only compatible with the $Q = 0$ momentum sector if N is even. For this reason, if N is odd this symmetry is absent, and the spectral statistics arise from a single GOE. It is also important to note that \mathcal{R}_{π} can only be defined when $k = \pi$ is an allowed wave vector in the ring. This places the additional constraint that L must be even. The presence of this symmetry thus precisely explains the conditions on GOE mixing observed in Fig. 7b.

Knowing this symmetry, it is thus possible to symmetrise the kinetically-driven BH Hamiltonian and divide it into two blocks, each block corresponding to one parity of \mathcal{R}_{π} . We show the results in Fig. 9. Clearly the results show that separating the two subspaces in this way indeed yields a single GOE distribution. In particular we note that the value of $\langle r \rangle$ now tends to the GOE value of 0.528 in the limit of large κ , exactly as we would expect. We can also see that the location of the crossover again shows a weak dependence on N , moving to a smaller value of κ as the system size is increased. As with the conventional BH model, this behaviour is broadly consistent with the transition occurring for an infinitesimal value of κ in the thermodynamic limit. But also like the conventional BH case, the precise behaviour of the Poisson-GOE crossover in the thermodynamic limit is an open question.

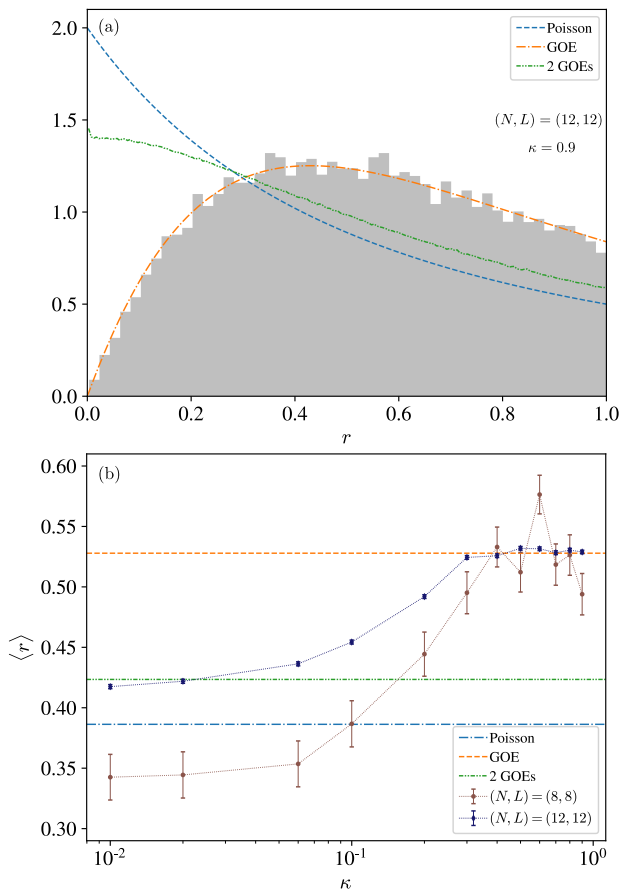


FIG. 9. Distribution of gap-ratios for the kinetically-driven BH model, applying the π -reflection symmetry to the effective Hamiltonian (7). (a) Previously (Fig. 6d) the distribution was a mixture of two GOEs. Applying the symmetry separates the two subspaces, so now the distribution is described by a single GOE. (b) Plotting the mean gap-ratio shows that the subspace of states indeed makes a transition from Poissonian statistics to the statistics of a single GOE as κ is increased.

IV. CONCLUSIONS

In summary, we have studied the spectral statistics of the Bose-Hubbard model under kinetic driving, and compared and contrasted its behaviour with that of the conventional BH model. When the driving parameter κ is small, the system lies in the Mott regime, and makes a transition to a superfluid behaviour as κ is increased. We have seen that, as also occurs in the conventional BH model, this transition is accompanied by a change in the spectral statistics: from Poisson to GOE. As a similar correlation between the nature of the ground state and the spectral statistics has also been seen previously in the conventional BH model [38], it is interesting to speculate that this somewhat unexpected link may be a general feature seen in systems tuned away from an integrable point. This may well be the case, at least for systems with

a superfluid ground state, because the same interactions that are needed to create a robust superfluid state [66, 67] can be expected to yield quantum chaos in the excited states. This correspondence is likely to be maintained in Bose systems with higher dimensions [68], for which integrability is less protected.

In contrast to the case of the conventional BH model, however, we have found that the form of the GOE statistics in the superfluid regime depends on the parities of the number of sites and the number of particles. When both of these quantities are even, evaluating the gap ratio of the spectrum has allowed us to establish that the system is accurately described as the mixture of two GOEs. We have further shown that this arises from an emergent symmetry we term “ π -reflection” invariance, produced by the kinetic driving. When this symmetry is not present, meaning that either N or L is odd, the system is described as a single GOE, characteristic of quantum chaos. We have thus seen how spectral statistics can be used as a probe to uncover hidden symmetries in a many-body quantum system.

Similarly to the case of the conventional BH model, the crossover in the spectral statistics from Poisson to GOE in the kinetically-driven BH model shows a weak dependence on the system size, moving towards smaller values of κ as the number of sites is increased. This behaviour is not inconsistent with the system making the transition to chaos for an infinitesimal symmetry breaking in the thermodynamic limit [69–72], although the existence of a finite threshold cannot be completely ruled out. A definitive statement would require a scaling analysis extending to much larger systems, which is computationally unfeasible at the current time, but remains an attractive prospect for future research.

ACKNOWLEDGMENTS

This work was supported by the the Spanish MICINN through Grant Nos. FIS2017-84368-P and PID2022-139288NB-100, and the Universidad Complutense de Madrid through Grant No. FEI-EU-19-12. The authors would like to thank Guillaume Roux for sharing eigenvalue data for the conventional BH model, and acknowledge stimulating and valuable conversations with Armando Relaño and Ángel Corps.

Appendix A: Symmetry and parity

For clarity of presentation, the results shown in Section III were restricted to just a few representative system sizes, namely (11, 12), (12, 12), (7, 8) and (8, 8). In Fig. 10 we give results for the kinetically-driven BH model for a more exhaustive selection of lattice sizes and particle numbers, to illustrate the parity dependence of the spectral statistics in the superfluid regime.

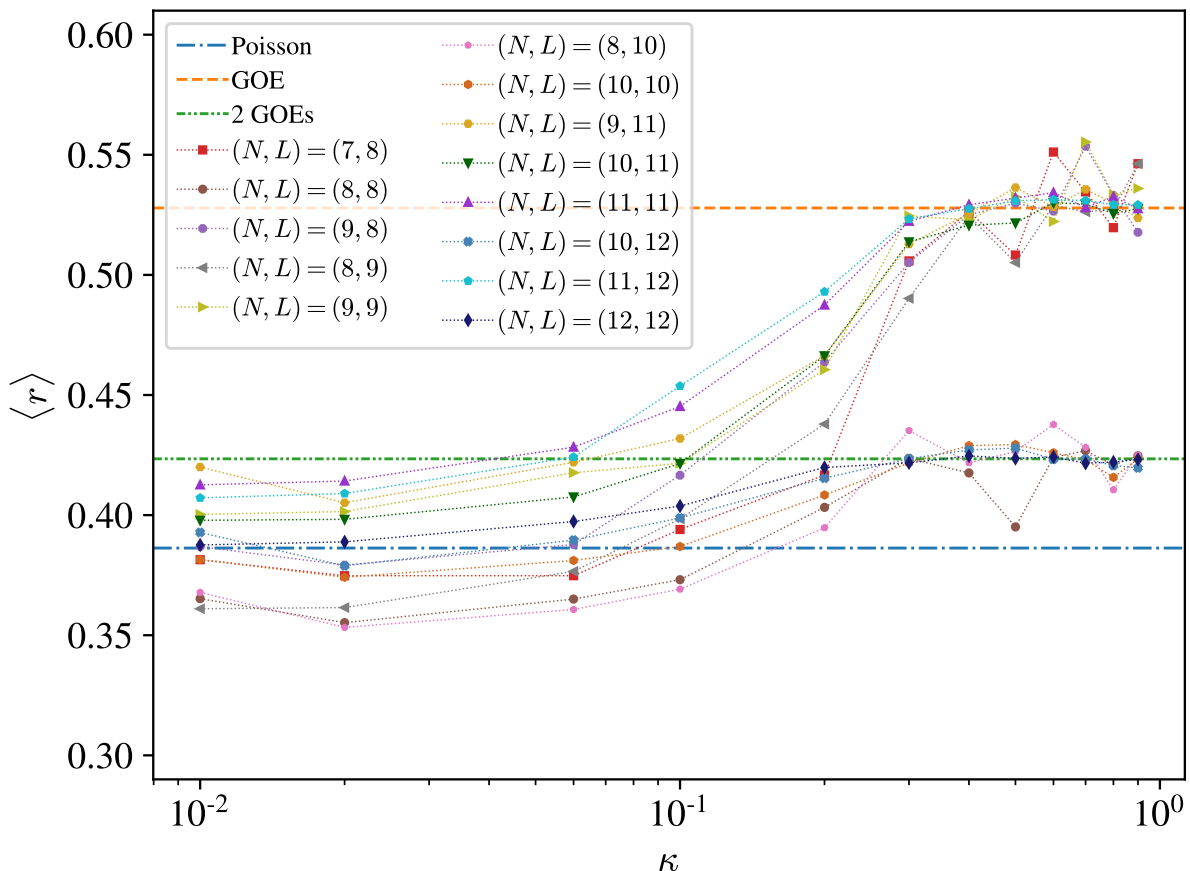


FIG. 10. Mean gap-ratio, $\langle r \rangle$ as a function of κ for a variety of choices of (N, L) . Two forms of behaviour are evident. For N and L both even, the distributions tend to a mixture of two GOEs as κ is increased. Conversely, if N or L is odd, the distribution tends towards a single GOE, in agreement with the symmetry analysis given in Section III C.

It is immediately clear that the curves fall into two distinct classes. In all cases the distributions tend towards being Poissonian in the limit $\kappa \rightarrow 0$. As κ is increased, one set of curves evolve toward the GOE result of $\langle r \rangle = 0.528$, while the remainder evolve towards the result for two mixed GOEs. This latter group corresponds to values of N and L which are both even, while those that evolve toward a single GOE have one or both of these quantities being odd.

This corresponds exactly to the symmetry dependence described in Section III C. If L is odd, then the momentum $k = \pi$ is not found in the FBZ, and so the π -reflection symmetry cannot be implemented. On the other hand, when N is odd, Eq. 15 is not invariant, and so the symmetry is absent. As a consequence, π -reflection symmetry is only realized in systems having both N and L even.

-
- [1] T. Oka and S. Kitamura, *Annual Review of Condensed Matter Physics* **10**, 387 (2019).
- [2] C. Weitenberg and J. Simonet, *Nature Physics* **17**, 1342 (2021).
- [3] D. H. Dunlap and V. M. Kenkre, *Phys. Rev. B* **34**, 3625 (1986).
- [4] H. Lignier, C. Sias, D. Ciampini, Y. Singh, A. Zenesini, O. Morsch, and E. Arimondo, *Phys. Rev. Lett.* **99**, 220403 (2007).
- [5] F. Grossmann, T. Dittrich, P. Jung, and P. Hänggi, *Phys. Rev. Lett.* **67**, 516 (1991).
- [6] M. Mitchell, A. Di Carli, G. Sinuco-León, A. La Rooij, S. Kuhr, and E. Haller, *Phys. Rev. Lett.* **127**, 243603 (2021).
- [7] P. Blanco-Mas and C. E. Creffield, *Phys. Rev. A* **107**, 043310 (2023).
- [8] D. Jaksch and P. Zoller, *New Journal of Physics* **5**, 56 (2003).
- [9] C. E. Creffield, G. Pieplow, F. Sols, and N. Goldman, *New Journal of Physics* **18**, 093013 (2016).

- [10] H. Miyake, G. A. Siviloglou, C. J. Kennedy, W. C. Burton, and W. Ketterle, *Phys. Rev. Lett.* **111**, 185302 (2013).
- [11] M. Aidelsburger, M. Atala, M. Lohse, J. T. Barreiro, B. Paredes, and I. Bloch, *Phys. Rev. Lett.* **111**, 185301 (2013).
- [12] M. Lewenstein, A. Sanpera, and V. Ahufinger, *Ultracold Atoms in Optical Lattices: Simulating quantum many-body systems* (OUP Oxford, 2012).
- [13] J. I. Cirac and P. Zoller, *Nature Physics* **8**, 264 (2012).
- [14] V. Borish, O. Marković, J. A. Hines, S. V. Rajagopal, and M. Schleier-Smith, *Phys. Rev. Lett.* **124**, 063601 (2020).
- [15] S. Geier, N. Thaicharoen, C. Hainaut, T. Franz, A. Salzinger, A. Tebben, D. Grimshandl, G. Zurn, and M. Weidemüller, *Science* **374**, 1149 (2021).
- [16] P. Scholl, H. J. Williams, G. Bornet, F. Wallner, D. Barredo, L. Henriot, A. Signoles, C. Hainaut, T. Franz, S. Geier, A. Tebben, A. Salzinger, G. Zürn, T. Lahaye, M. Weidemüller, and A. Browaeys, *PRX Quantum* **3**, 020303 (2022).
- [17] M. Gilowski, T. Wendrich, T. Müller, C. Jentsch, W. Ertmer, E. M. Rasel, and W. P. Schleich, *Phys. Rev. Lett.* **100**, 030201 (2008).
- [18] R. He, M.-Z. Ai, J.-M. Cui, Y.-F. Huang, Y.-J. Han, C.-F. Li, G.-C. Guo, G. Sierra, and C. E. Creffield, *npj Quantum Information* **7**, 109 (2021).
- [19] A. Eckardt, C. Weiss, and M. Holthaus, *Phys. Rev. Lett.* **95**, 260404 (2005).
- [20] C. E. Creffield and T. S. Monteiro, *Phys. Rev. Lett.* **96**, 210403 (2006).
- [21] A. Lazarides, A. Das, and R. Moessner, *Phys. Rev. E* **90**, 012110 (2014).
- [22] L. D’Alessio and M. Rigol, *Phys. Rev. X* **4**, 041048 (2014).
- [23] D. A. Abanin, W. De Roeck, W. W. Ho, and F. m. c. Huveneers, *Phys. Rev. B* **95**, 014112 (2017).
- [24] D. A. Abanin, W. De Roeck, and F. m. c. Huveneers, *Phys. Rev. Lett.* **115**, 256803 (2015).
- [25] T. Mori, T. Kuwahara, and K. Saito, *Phys. Rev. Lett.* **116**, 120401 (2016).
- [26] D. Abanin, W. De Roeck, W. W. Ho, and F. Huveneers, *Communications in Mathematical Physics* **354**, 809 (2017).
- [27] P. Weinberg, M. Bukov, L. D’Alessio, A. Polkovnikov, S. Vajna, and M. Kolodrubetz, *Physics Reports* **688**, 1 (2017).
- [28] R. Peña, V. M. Bastidas, F. Torres, W. J. Munro, and G. Romero, *Phys. Rev. B* **106**, 064307 (2022).
- [29] M. V. Berry and M. Tabor, *Proc. R. Soc. Lond. A* **356**, 375 (1977).
- [30] O. Bohigas, M. J. Giannoni, and C. Schmit, *Phys. Rev. Lett.* **52**, 1 (1984).
- [31] M. Faas, B. D. Simons, X. Zotos, and B. L. Altshuler, *Phys. Rev. B* **48**, 5439 (1993).
- [32] K. Kudo and T. Deguchi, *Phys. Rev. B* **68**, 052510 (2003).
- [33] L. Benet, F. Leyvraz, and T. H. Seligman, *Phys. Rev. E* **68**, 045201 (2003).
- [34] A. Relaño, J. Dukelsky, J. M. G. Gómez, and J. Retamosa, *Phys. Rev. E* **70**, 026208 (2004).
- [35] D. Poilblanc, T. Ziman, J. Bellissard, F. Mila, and G. Montambaux, *Europhysics Letters* **22**, 537 (1993).
- [36] T. C. Hsu and J. C. Angle’s d’Auriac, *Phys. Rev. B* **47**, 14291 (1993).
- [37] A. R. Kolovsky and A. Buchleitner, *Europhysics Letters* **68**, 632 (2004).
- [38] C. Kollath, G. Roux, G. Biroli, and A. M. Läuchli, *Journal of Statistical Mechanics: Theory and Experiment* **2010**, P08011 (2010).
- [39] J. De Marco, L. Tolle, C.-M. Halati, A. Sheikhan, A. M. Läuchli, and C. Kollath, *Phys. Rev. Res.* **4**, 033119 (2022).
- [40] M. Haque and P. A. McClarty, *Phys. Rev. B* **100**, 115122 (2019).
- [41] G. Pieplow, F. Sols, and C. E. Creffield, *New Journal of Physics* **20**, 073045 (2018).
- [42] S. D. Huber and E. Altman, *Phys. Rev. B* **82**, 184502 (2010).
- [43] H.-Y. Hui, Y. Zhang, C. Zhang, and V. W. Scarola, *Phys. Rev. A* **95**, 033603 (2017).
- [44] J. Zurita, C. E. Creffield, and G. Platero, *Advanced Quantum Technologies* **3**, 1900105 (2020).
- [45] M. Hyrkäs, V. Apaja, and M. Manninen, *Phys. Rev. A* **87**, 023614 (2013).
- [46] S. Takayoshi, H. Katsura, N. Watanabe, and H. Aoki, *Phys. Rev. A* **88**, 063613 (2013).
- [47] M. Tovmasyan, S. Peotta, L. Liang, P. Törmä, and S. D. Huber, *Phys. Rev. B* **98**, 134513 (2018).
- [48] Y. Kuno, T. Mizoguchi, and Y. Hatsugai, *Phys. Rev. A* **102**, 063325 (2020).
- [49] G. Pelegrí, A. M. Marques, V. Ahufinger, J. Mompart, and R. G. Dias, *Phys. Rev. Res.* **2**, 033267 (2020).
- [50] G. Pieplow, C. E. Creffield, and F. Sols, *Phys. Rev. Res.* **1**, 033013 (2019).
- [51] J. Mateos, C. E. Creffield, and F. Sols, *New Journal of Physics* **25**, 063006 (2023).
- [52] For ease of notation we use the term “superfluid”, although in one dimension a system cannot have true long-range order. This, however, is not an important limitation in realistic finite-size systems.
- [53] M. A. Cazalilla, R. Citro, T. Giamarchi, E. Orignac, and M. Rigol, *Rev. Mod. Phys.* **83**, 1405 (2011).
- [54] S. Blanes, F. Casas, J. Oteo, and J. Ros, *Physics Reports* **470**, 151 (2009).
- [55] A. Eckardt and E. Anisimovas, *New Journal of Physics* **17**, 093039 (2015).
- [56] A. Zenesini, H. Lignier, D. Ciampini, O. Morsch, and E. Arimondo, *Phys. Rev. Lett.* **102**, 100403 (2009).
- [57] O. Dutta, M. Gajda, P. Hauke, M. Lewenstein, D.-S. Lühmann, B. A. Malomed, T. Sowiński, and J. Zakrzewski, *Reports on Progress in Physics* **78**, 066001 (2015).
- [58] J. M. G. Gómez, R. A. Molina, A. Relaño, and J. Retamosa, *Phys. Rev. E* **66**, 036209 (2002).
- [59] As H_{eff} is obtained by a Floquet method, we must also ensure that ω is sufficiently large for all the quasienergies to lie in the first quasienergy Brillouin zone. If not, some quasienergies will wrap around the Brillouin zone, and the system will instead be described by the circular orthogonal ensemble. As we work in the high-frequency regime, $\omega \gg U$, this condition is amply satisfied.
- [60] V. Oganesyan and D. A. Huse, *Phys. Rev. B* **75**, 155111 (2007).
- [61] Y. Y. Atas, E. Bogomolny, O. Giraud, and G. Roux, *Phys. Rev. Lett.* **110**, 084101 (2013).
- [62] A. L. Corps and A. Relaño, *Phys. Rev. E* **101**, 022222 (2020).

- [63] This quantity cannot be calculated analytically, and the various surmises provide different estimates of its value, which, however, only differ by a few percent. In this paper we make use of the values given in Ref. [62].
- [64] N. Rosenzweig and C. E. Porter, *Phys. Rev.* **120**, 1698 (1960).
- [65] O. Giraud, N. Macé, E. Vernier, and F. Alet, *Phys. Rev. X* **12**, 011006 (2022).
- [66] A. J. Leggett, *Quantum Liquids: Bose condensation and Cooper pairing in condensed-matter systems* (Oxford University Press, 2006).
- [67] M. Heimsoth, C. E. Creffield, L. D. Carr, and F. Sols, *New Journal of Physics* **14**, 075023 (2012).
- [68] D. Fischer, D. Hoffmann, and S. Wimberger, *Phys. Rev. A* **93**, 043620 (2016).
- [69] D. A. Rabson, B. N. Narozhny, and A. J. Millis, *Phys. Rev. B* **69**, 054403 (2004).
- [70] M. Rigol and L. F. Santos, *Phys. Rev. A* **82**, 011604 (2010).
- [71] L. F. Santos and M. Rigol, *Phys. Rev. E* **81**, 036206 (2010).
- [72] L. F. Santos, F. Pérez-Bernal, and E. J. Torres-Herrera, *Phys. Rev. Res.* **2**, 043034 (2020).